

Dartmouth College Dartmouth Digital Commons

Open Dartmouth: Faculty Open Access Articles

1997

Matching Numerical Simulations to Continuum Field Theories: A Lattice Renormalization Study

J Borrill

Dartmouth College

M. Gleiser

Dartmouth College

Follow this and additional works at: <https://digitalcommons.dartmouth.edu/facoa>



Part of the [Nuclear Commons](#)

Recommended Citation

J Borrill and Gleiser, M., "Matching Numerical Simulations to Continuum Field Theories: A Lattice Renormalization Study" (1997).
Open Dartmouth: Faculty Open Access Articles. 2458.
<https://digitalcommons.dartmouth.edu/facoa/2458>

This Article is brought to you for free and open access by Dartmouth Digital Commons. It has been accepted for inclusion in Open Dartmouth: Faculty Open Access Articles by an authorized administrator of Dartmouth Digital Commons. For more information, please contact dartmouthdigitalcommons@groups.dartmouth.edu.

Matching numerical simulations to continuum field theories: A lattice renormalization study

Julian Borrill and Marcelo Gleiser^{*†}

Department of Physics and Astronomy, Dartmouth College, Hanover, NH 03755

(May 9, 2018)

The study of nonlinear phenomena in systems with many degrees of freedom often relies on complex numerical simulations. In trying to model realistic situations, these systems may be coupled to an external environment which drives their dynamics. For nonlinear field theories coupled to thermal (or quantum) baths, discrete lattice formulations must be dealt with extreme care if the results of the simulations are to be interpreted in the continuum limit. Using techniques from renormalization theory, a self-consistent method is presented to match lattice results to continuum models. As an application, symmetry restoration in ϕ^4 models is investigated.

PACS: 64.60.Cn, 05.50.+q, 11.10.Gh

arXiv:hep-lat/9607026v1 9 Jul 1996

^{*}NSF Presidential Faculty Fellow

[†]email: borrill@neville.dartmouth.edu, gleiser@peterpan.dartmouth.edu

The study of nonlinear phenomena has changed dramatically during the last two decades or so, as an increasing number of once forbidding problems have become amenable to treatment by faster and cheaper computers. From coupled anharmonic oscillators to gravitational clustering, from plasma physics to the dynamics of phase transitions, numerical simulations are often the only tool to probe the physics of complex nonlinear systems [1].

Typically, we are interested in investigating the behavior of a particular physical system described by ordinary or partial nonlinear differential equations. In the present work, focus will be mostly on the latter case, which can be thought of as representing systems with finitely or infinitely many coupled degrees of freedom. Apart from very few exceptions, such as kink solutions for sine-Gordon or ϕ^4 models [2], nonlinear partial differential equations have no analytical solutions. The situation is even worse if we attempt to model realistic behavior by coupling the system to an external environment. This external environment often represents a thermal or quantum bath, adding an element of stochasticity to the deterministic evolution equations. In order to gain some insight into the role of nonlinearities, perturbation theory is frequently used. However, examples ranging from the simple pendulum equation [3] to critical phenomena during phase transitions [4] remind us that perturbation theory breaks down precisely in the region of parameter space where nonlinear effects become predominant.

The alternative is to address the problem numerically, solving the equations of interest using a computer. In the case of partial differential equations, the problem is set up on a lattice which represents a particular choice of discretization procedure. For a function of d -dimensional position and time, $f(\mathbf{x}, t)$, satisfying some partial differential equation with given initial and boundary conditions, we typically construct a d -dimensional lattice of a given geometry, say cubic or triangular, to represent space at a particular instant, and replicate it at (usually regular) intervals to represent time. The continuous function may then be discretized following well-prescribed rules by which continuous derivatives are approximated by finite ratios of the lattice variables [5].

The use of a spatial lattice introduces two artificial length scales; the ‘macroscopic’ size

of the lattice in each dimension, L , and the ‘microscopic’ distance between neighbouring lattice points, δx . These length scales provide bounds on the wavelengths of modes which can be represented on the lattice, whilst the total the number of lattice points N (for cubic lattices being $N = (L/\delta x)^d$) is the restricted number of degrees of freedom being integrated at each time step. Computational physicists (and computers) spend a considerable amount of time trying to get around the limitations that these length scales introduce to numerical studies of continuum systems. Occasionally, one or other of these limitations may become insignificant due to the particular physical behavior of the system; for example, close to the critical point of a second order phase transition the divergence of the characteristic length scale of the system means that its bulk properties (and in particular its critical exponents) are determined by the long wavelength modes alone, doing away with the need for the high spatial resolution given by a small lattice spacing δx [4]. In general, however, since the continuum corresponds to the limit $L \rightarrow \infty, \delta x \rightarrow 0, N \rightarrow \infty$, a better approximation is obtained from a larger and finer lattice, leading to the notion of the continuum limit of a discrete system. For continuum systems described by continuous functions, such as fluids, fields, or deformable bodies, our discrete representation should have a well-defined continuum limit, *i.e.*, one that is stable as $\delta x \rightarrow 0$ (at fixed L). Moreover, we should also demand that it is a *good* continuum limit, in that it matches the original continuum system. As discussed below, for systems coupled to external environments, even if the continuum limit can be achieved on the lattice it is not always clear how to match the lattice results to a continuum theory. These two questions — how to achieve a continuum limit in lattice simulations, and how to ensure that it is a good limit, in the sense of matching the appropriate continuum theory — are the focus of this work.

For linear systems, achieving a continuum limit does not usually present any difficulties. Typically there is a minimal length-scale in the problem which can be used as a guideline for the choice of δx . For example, when solving the wave equation, it is possible to find a small enough δx and show that the same results are obtained if smaller values are used, provided

one makes sure the discretization of time is appropriately chosen so that the evolution is stable.

For nonlinear systems, the situation is more complicated. If we think for a moment in terms of a Fourier decomposition of the function $f(\mathbf{x}, t)$, the effect of nonlinearities is to couple different wavelength modes in a nontrivial way; the dynamics of short wavelength modes will influence the dynamics of long wavelength modes and *vice-versa*. Mechanisms to handle this problem are sensitive both to the particular system under study and to which of its properties are of interest, often seeming to be more an art than a science. For example, if we are solely interested in the dynamics of long wavelength modes with slow relaxation time-scales, it may be possible to add extra artificial terms to the evolution equations which damp the behavior of faster modes. For situations in which nonlinear fields are coupled to an external environment with stochastic properties, say a thermal (or quantum) bath, a detailed investigation of how to approach the continuum limit on the lattice is lacking. This does not imply that this problem has been completely overlooked, but that it may have received less attention than it deserves.

In the context of classical field theories at finite temperature there has been some work on obtaining such a continuum limit. For example, Parisi [6] suggested the addition of renormalization counterterms, a proposal then implemented by Alford and Gleiser [7] in the context of 2-dimensional nucleation studies (albeit with a somewhat *ad hoc* match to a continuum theory), and by Kajantie *et al.* [8] in lattice gauge simulations of the electroweak phase transition. Alford and Gleiser in particular showed that neglecting lattice spacing effects in the numerical determination of nucleation rates can lead to severe errors in the measured values. This conclusion is not particular to systems exhibiting metastable states, but to any nonlinear field model in contact with external stochastic environments. Thus, the issues that are raised here are of concern to a wide range of physical systems modelled through the separation of system and environment, from quantum field theories to effective field theories describing condensed matter systems.

Even if a continuum limit can be achieved on the lattice, we must still ensure that the numerical results correspond to the appropriate continuum theory. In general, the coupling to a stochastic environment modifies the effective lattice theory, which cannot be naively matched to the original continuum model. The question then becomes what theory is the lattice simulating, and can we extract it in a self-consistent way? These questions will be addressed below in the context of two continuous nonlinear models in 2+1 dimensions, one temperature independent and the other temperature dependent (the well-known Ginzburg-Landau model). Both models describe phase transitions in the Ising universality class. Extensions to $d + 1$ dimensions should be straightforward.

Formulating continuum models on a lattice: The issues

Consider a single scalar field $\phi(\mathbf{x}, t)$ in a potential $V_0(\phi)$ which may or not be temperature dependent. This potential can model interactions of ϕ with itself and with other fields. For example, a linear term of the form $\phi\mathcal{H}$ is often used to represent the coupling of ϕ to an external magnetic field for models of ferromagnetic transitions. In this report, focus will be on potentials which are simple polynomials of even power in ϕ , although our approach is equally valid for potentials with odd powers of ϕ , typical of nucleation studies. The Hamiltonian for this system is, (in units of $c = k_B = 1$)

$$\frac{H[\phi]}{T} = \frac{1}{T} \int d^2x \left[\frac{1}{2} (\nabla\phi \cdot \nabla\phi) + V_0(\phi) \right] . \quad (1)$$

The field ϕ can be thought of as representing a scalar order parameter in models of phase transitions in the Ising universality class, such as ferromagnets, binary fluid mixtures, metal alloys, or in studies of domain wall formation in cosmology. As such, it is convenient to model its dynamics in contact with a heat bath by means of a generalized Langevin equation,

$$\frac{\partial^2\phi}{\partial t^2} = \nabla^2\phi - \eta \frac{\partial\phi}{\partial t} - \frac{\partial V_0}{\partial\phi} + \xi(\mathbf{x}, t) , \quad (2)$$

where the viscosity coefficient η is related to the stochastic force of zero mean $\xi(\mathbf{x}, t)$ by the fluctuation-dissipation relation,

$$\langle \xi(\mathbf{x}, t) \xi(\mathbf{x}', t') \rangle = 2\eta T \delta(\mathbf{x} - \mathbf{x}') \delta(t - t') . \quad (3)$$

This approach guarantees that ϕ will be driven into equilibrium, although the time-scale η^{-1} is arbitrary. It has been extensively used in numerical simulations of thermal creation of kink-antikink pairs [9], nucleation [7,10], spinodal decomposition [11], and pattern formation in the presence of external noise [12], to mention but a few examples. Note that in the high viscosity limit the second-order time derivative can be neglected, as is common practice in systems with slower dynamical time-scales.

The next step is to discretize this system and cast it on a lattice. Using a standard second-order staggered leapfrog method we can write,

$$\begin{aligned} \dot{\phi}_{i,m+1/2} &= \frac{(1 - \frac{1}{2}\eta\delta t)\dot{\phi}_{i,m-1/2} + \delta t(\nabla^2\phi_{i,m} - V'_0(\phi_{i,m}) + \xi_{i,m})}{1 + \frac{1}{2}\eta\delta t} \\ \phi_{i,m+1} &= \phi_{i,m} + \delta t\dot{\phi}_{i,m+1/2} \end{aligned} \quad (4)$$

where i -indices are spatial and m -indices temporal, overdots represent derivatives with respect to t and primes with respect to ϕ . The discretised fluctuation-dissipation relation now reads

$$\langle \xi_{i,m} \xi_{j,n} \rangle = 2\eta T \frac{\delta_{i,j}}{\delta x^2} \frac{\delta_{m,n}}{\delta t} \quad (5)$$

so that

$$\xi_{i,m} = \sqrt{\frac{2\eta T}{\delta x^2 \delta t}} G_{i,m} \quad (6)$$

where $G_{i,m}$ is taken from a zero-mean unit-variance Gaussian.

Note that as a first guess we have used $V_0(\phi)$ in the lattice formulation of the model. Is this the correct procedure? It is well-known that classical field theory in more than one spatial dimension is ultraviolet divergent, the Rayleigh-Jeans ultraviolet catastrophe [13]. Formulating the theory on a lattice takes care of the problem, as a sharp momentum cutoff is introduced by the lattice spacing δx , with $\Lambda = \pi/\delta x$. However, a finite lattice spacing creates two difficulties. First, the lattice theory is coarse-grained on the scale δx ; in other words, the lattice theory is not equivalent to the continuum theory we started with, and our results

will depend on δx , unless this dependence is handled by a proper renormalization procedure. Second, if the lattice theory is not equivalent to the continuum theory we started with, to what continuum theory is it equivalent to? Fortunately, there is a well-defined procedure that addresses both difficulties at once. Within its validity, it is possible to establish a one-to-one correspondence between lattice simulations and field theories in contact with stochastic baths.

Formulating continuum models on a lattice: The procedure

In order to recover the continuum limit on the lattice we must eliminate any dependence on the cutoff. The coupling to the heat bath will induce fluctuations on all possible scales. Since the cutoff sets the scale for the smallest possible spatial fluctuations in the system, we may incorporate the effects of all fluctuations down to the smallest scale using perturbation theory. Thus, the lattice theory must be equivalent to a continuum theory with a sharp ultraviolet cutoff. For classical field theories, the one-loop corrected effective potential with a large momentum cutoff is given by [14],

$$V_{\text{1L}}(\phi) = V_0 + \frac{T}{2} \int_0^\Lambda \frac{d^2 p}{(2\pi)^2} \ln(p^2 + V_0'') + \text{counterterms} . \quad (7)$$

These theories describe fluctuations with $\hbar\omega \ll k_B T$. In semi-classical language, the excitations of the field contain many fundamental quanta. Note that there is a one-to-one correspondence between classical statistical field theory in $d + 1$ dimensions and Euclidean quantum field theory in d dimensions. While the loop expansion is in powers of T for the former, it is in powers of \hbar for the latter. For $d = 2$, the only divergences are at one loop, although higher loops can generate finite terms which modify the effective Hamiltonian. The dependence on the cutoff Λ can be handled by introducing proper counterterms.

Integration gives,

$$V_{\text{1L}}(\phi) = V_0 + \frac{T}{8\pi} V_0'' \left[1 - \ln \left(\frac{V_0''}{\Lambda^2} \right) \right] + \text{counterterms} . \quad (8)$$

The form of V_0 will determine the counterterms needed to cancel the dependence on Λ . For polynomial potentials of order ϕ^n , one typically needs counterterms up to order ϕ^{n-2} . In

the case of interest here, degenerate double-well potentials, only one quadratic counterterm is needed, of form $a\phi^2$, with a constant. As usual, the value of a is fixed by imposing a renormalization condition. Because of the logarithmic divergence, the renormalization condition must be imposed at some energy scale M , which is chosen to be,

$$V_{\text{1L}}''(\phi = \sqrt{M}) = V_0''(\phi = \sqrt{M}) . \quad (9)$$

The renormalized one-loop corrected potential is then,

$$V_{\text{1L}}(\phi) = V_0 + \frac{T}{8\pi} V_0'' \left[1 - \ln \left(\frac{V_0''}{\Lambda^2} \right) \right] + \frac{T}{16\pi} \left(V_0'''' \ln \left(\frac{V_0''}{\Lambda^2} \right) + \frac{(V_0''')^2}{V_0''} \right) \Big|_{\phi=\sqrt{M}} \phi^2 \quad (10)$$

The above procedure incorporates thermal fluctuations to the original potential $V_0(\phi)$ at some energy scale M to one-loop order. As with any perturbative approach, it will break down wherever large amplitude fluctuations are present, and in particular close to the critical point T_c . Although there are techniques to improve the perturbative expansion in the neighborhood of the critical point, such as ε -expansion methods [15] (not too reliable for 2-d), in this work we will concentrate on the matching of the continuum theory to the lattice simulation in regions of the parameter space where the one-loop calculation is valid. Close to criticality the theory of Eq. 10 breaks down, and we restrict our investigation to the extraction of the critical exponent controlling the divergence of the order parameter.

How is this continuum theory matched to the lattice simulation? The procedure we propose is quite simple. Since the continuum theory above incorporates fluctuations from momentum scales up to Λ , we write the lattice potential as,

$$V_{\text{latt}}(\phi) = V_0 + a\phi^2 , \quad (11)$$

where a is fixed by the renormalization condition in the continuum, but with $\Lambda = \pi/\delta x$.

That is,

$$V_{\text{latt}}(\phi) = V_0 + \frac{T}{16\pi} \left(V_0'''' \ln \left(\frac{V_0''}{(\pi/\delta x)^2} \right) + \frac{(V_0''')^2}{V_0''} \right) \Big|_{\phi=\sqrt{M}} \phi^2 . \quad (12)$$

As we show below, this procedure takes care of the two problems raised by formulating the continuum theory on the lattice, namely, the dependence of lattice results on lattice spacing

and the matching of the lattice theory to the continuum at some renormalization energy scale M . The generic emergence of a good continuum limit from Eq. 12 is the central result of this work.

Applications

We will apply the above procedure to two cases, with potentials which are temperature independent and temperature dependent, respectively. Consider first the temperature-independent potential,

$$V_0(\phi) = -\frac{1}{2}m^2\phi^2 + \frac{1}{4}\lambda\phi^4 . \quad (13)$$

Choosing the renormalization point to be $\phi_{RN} = \sqrt{\frac{M^2+m^2}{3\lambda}}$, the renormalized continuum potential is, from Eq. 10,

$$V_{\text{IL}}(\phi) = -\frac{1}{2}m^2\phi^2 + \frac{1}{4}\lambda\phi^4 + \frac{3\lambda T}{8\pi} \left(1 + 2 \frac{M^2 + m^2}{M^2} \right) \phi^2 - \frac{T}{8\pi} (3\lambda\phi^2 - m^2) \ln \left(\frac{3\lambda\phi^2 - m^2}{M^2} \right) . \quad (14)$$

It is convenient to introduce dimensionless variables (because there is no \hbar in this theory, m has dimensions of $(\text{length})^{-1}$ while ϕ has dimensions of $(\text{energy})^{1/2}$), $\tilde{x} = xm$, $\tilde{t} = tm$, $\tilde{\phi} = \phi\lambda^{1/2}m^{-1}$, $\tilde{\eta} = \eta m^{-1}$, $\theta = T\lambda m^{-2}$, $\tilde{M} = Mm^{-1}$, $\tilde{\Lambda} = \Lambda m^{-1}$. From the discussion in the previous section, the lattice-spacing independent lattice potential is, using dimensionless variables (and dropping the tildes),

$$V_{\text{latt}}(\phi) = -\frac{1}{2}\phi^2 + \frac{1}{4}\phi^4 + \frac{3\theta}{4\pi} \left(\ln \left(\frac{M\delta x}{\pi} \right) + \frac{M^2 + 1}{M^2} \right) \phi^2 . \quad (15)$$

Fig. 1 shows the impact of the added counterterm to the lattice results. We display the time evolution of the spatially averaged field, $\bar{\phi} = \frac{1}{A} \int dA\phi$, starting from a broken symmetric phase $\bar{\phi} = -1$, without the counterterm (Fig. 1a) and with the counterterm (Fig. 1b). The parameters θ , M , and physical lattice size L , were kept fixed, and only the lattice spacing δx was varied. (Throughout this work we keep the viscosity coefficient $\eta = 1$ as we are only interested in final equilibrium quantities.) Clearly, omitting the counterterm leads

to severe lattice spacing dependence of the results, even to the point of having symmetry restoration. Experiments varying θ and M showed that the procedure is robust, with excellent δx -independence being achieved, even close the critical point, as long as the expansion parameter $\theta/8\pi \ll 1$.

The next step is to compare the lattice results with the continuum models of Eq. 14 in their domain of validity. Being perturbative, we expect the continuum models to break down when the fluctuations become large, at high temperatures or close to the critical point. By contrast, the lattice models incorporate fluctuations up to the limiting size L , and so may remain valid even when the continuum models break down. The continuum potential gives a prediction for the critical temperature of

$$\theta_c = \frac{2\pi}{3(1 + M^{-2} + \ln M)} . \quad (16)$$

Note that θ_c has its maximum value at $M^2 = 2$; as we move away from this point in either direction θ_c decreases, and we should expect perturbation theory to continue to be a valid approximation closer and closer to the critical point. Ultimately, however, the phase transition is nonperturbative, the field fluctuations become large, and perturbation theory must fail. Fig. 2 shows the variation in the equilibrium mean field value $\bar{\phi}_{\text{eq}}$ with temperature θ , squares from the lattice and lines from the continuum, for values of the renormalization energy-scale $M = 0.1$ (Fig. 2a), $M = \sqrt{2}$ (Fig. 2b), and $M = 10$ (Fig. 2c). The discontinuities in the continuum are related to the concavity of the corrected potential between the inflection points, which gives rise to an imaginary part. As shown by Weinberg and Wu [16], the imaginary part of the potential represents unstable physical states typical of the process of phase separation; the figure shows only the real part of the corrected potential. There is indeed excellent agreement at low temperatures, which is progressively lost as the temperature increases.

At the one-loop level, perturbation theory is equivalent to mean field theory. Close to the critical point, where mean field theory breaks down, we expect the equilibrium value of $\bar{\phi}$ to diverge as a power law,

$$\bar{\phi}_{\text{eq}} \propto \left(\frac{\theta_c - \theta}{\theta_c} \right)^\beta \quad (17)$$

with the critical exponent $\beta = 1/2$ for mean field theory and $\beta = 1/8$ for the 2-d Ising model. Figure 3 shows the behavior of the lattice and continuum equilibrium mean field values $\bar{\phi}_{\text{eq}}$ with reduced temperature $\theta_r \equiv (\theta_c - \theta)/\theta_c$ for $M = 0.1$ — squares being results from the lattice simulations, triangles the predicted behavior from the continuum, and the lines indicating the two slopes $\beta = 1/2$ and $\beta = 1/8$. We see that the continuum perturbation theory behaves as a mean field theory, whilst the lattice theory in the neighborhood of the critical point is in the universality class of the 2-d Ising model as expected.

We now consider the case of a temperature-dependent potential. The goal is to show that the above procedure works equally well in this case; both lattice-spacing independence and the matching to a continuum theory can be achieved in a consistent way. Coupling a temperature-dependent potential to a heat bath does not necessarily imply a double counting of the thermal degrees of freedom. The choice of potential V_0 simply reflects different physical models. For example, one may include phenomenological temperature-dependent terms in V_0 , as in the Ginzburg-Landau model, or may obtain temperature corrections by integrating out from the partition function either other fields coupled to ϕ or short wavelength modes of the field ϕ itself [17]. In either case, the heat bath may then be representing stochastic forces not included in the integration process, or simply an external environment coupled to ϕ phenomenologically, which drives the system to its final equilibrium state. As an example, we choose the Ginzburg-Landau potential,

$$V_0(\phi) = \frac{1}{2}a(T - T'_c)\phi^2 + \frac{1}{4}\lambda\phi^4, \quad (18)$$

where the prime is a reminder that the critical temperature has an arbitrary value in the mean field model. Fixing the renormalization energy scale at $\phi_{RN} = \sqrt{\frac{M^2 - a(T - T'_c)}{3\lambda}}$, the renormalized continuum potential becomes,

$$V_{\text{IL}}(\phi) = \frac{1}{2}a(T - T'_c)\phi^2 + \frac{1}{4}\lambda\phi^4 + \frac{3\lambda T}{8\pi} \left(1 + 2 \frac{M^2 - a(T - T'_c)}{M^2} \right) \phi^2$$

$$-\frac{T}{8\pi} [3\lambda\phi^2 + a(T - T'_c)] \ln \left(\frac{3\lambda\phi^2 + a(T - T'_c)}{M^2} \right). \quad (19)$$

Following the same steps as before and arbitrarily setting $\theta'_c = 1$, this theory is matched on the lattice to

$$V_{\text{latt}}(\phi) = \frac{1}{2}(\theta - 1)\phi^2 + \frac{1}{4}\phi^4 + \frac{3\theta}{4\pi} \left[\ln \left(\frac{M\delta x}{\pi} \right) + \frac{M^2 - (\theta - 1)}{M^2} \right] \phi^2. \quad (20)$$

Fig. 4 compares the lattice results without (Fig. 4a) and with (Fig. 4b) the renormalization counterterm. The prescription to obtain lattice-spacing independence works equally well in this case. Fig. 5 again compares the lattice simulations (squares) and the continuum model (lines) for renormalization scales $M = 0.1$ (Fig. 5a), $M = \sqrt{2}$ (Fig. 5b), and $M = 10$ (Fig. 5c). For low temperatures excellent agreement is obtained, as in the temperature independent case. Note that this also confirms that our model has not been ‘twice-cooked’; had it been, no such agreement would be possible. Finally, in Fig. 6, we show the critical behavior of the lattice (squares) and continuum (triangles) for $M = 0.1$. Again the lattice obtains the Ising critical exponent, $\beta = 1/8$, close to criticality.

In summary, we have presented a self-consistent method to match lattice simulations to nonlinear field theories in contact with an external stochastic environment. This approach is of potential interest in a wide range of physical problems, from noise-induced pattern-forming instabilities and phase separation in condensed matter physics to symmetry breaking in high energy physics and cosmology. It was shown that adding the right renormalization counterterms to the lattice potential provides a good continuum limit, independent of the lattice-spacing and matching the appropriate continuum theory. That this matching breaks down at high temperatures and/or close to a critical point is not surprising, as it reflects the limitations of perturbation theory in probing critical phenomena quantitatively. The procedure was demonstrated to work well for a large class of widely-used potentials — both temperature independent and dependent — and over a wide range of the renormalization energy scale M .

- [1] Introductions to numerical methods in physics can be found in P. L. DeVries, *A First Course in Computational Physics*, (John Wiley & Sons, New York, 1994); D. W. Heermann, *Computer Simulation Methods in Theoretical Physics*, (Springer-Verlag, Berlin, 1990).
- [2] See, e.g., R. K. Dodd, J. C. Eilbeck, J. D. Gibbon, H. C. Morris, *Solitons and Nonlinear Wave Equations*, (Academic, New York, 1982).
- [3] H. Goldstein, *Classical Mechanics*, 2nd Ed., (Addison-Wesley, Reading, Massachusetts, 1980).
- [4] N. Goldenfeld, *Lectures on Phase Transitions and the Renormalization Group*, Frontiers in Physics, vol. 85, (Addison-Wesley, New York, 1992).
- [5] W. H. Press, S. A. Teukolsky, W. T. Vetterling, and B. P. Flannery, *Numerical Recipes*, 2nd Ed. (Cambridge University Press, New York, 1992).
- [6] G. Parisi, *Statistical Field Theory* (Addison-Wesley, New York, 1988).
- [7] M. Alford and M. Gleiser, Phys. Rev. D**48**, 2838 (1993).
- [8] K. Kajantie, M. Laine, K. Rummukainen, and M. Shaposhnikov, Nucl. Phys. B**458**, 90 (1996); D. Bodeker, L. McLerran, and A. Smilga, Phys. Rev. D**52**, 4675 (1995).
- [9] M. Alford, H. Feldman, and M. Gleiser, Phys. Rev. Lett. **68**, 1645 (1992); F. J. Alexander and S. Habib, Phys. Rev. Lett. **71**, 955 (1993).
- [10] M. Alford, H. Feldman, and M. Gleiser, Phys. Rev. D**47** (RC), 2168 (1993); O. T. Valls and G. F. Mazenko, Phys. Rev. B**42**, 6614 (1990); for a review see, J. D. Gunton, M. San Miguel and P. S. Sahni, in *Phase Transitions and Critical Phenomena*, Vol. **8**, Ed. C. Domb and J. L. Lebowitz (Academic Press, London, 1983).
- [11] See, for example, M. Schöbinger, S. W. Koch, and F. F. Abraham, J. Stat. Phys. **42**, 1071 (1986); M. Laradji, M. Grant, M. J. Zuckerman, and W. Klein, Phys. Rev. B**41**, 4646 (1990); R. Toral and A. Chakrabarti, Phys. Rev. B**42**, 2445 (1990).
- [12] C. R. Doering, H. R. Brand and R. E. Ecke, eds. *External Noise and Its Interaction with*

- Spatial Degrees of Freedom in Nonlinear Dissipative Systems*, Workshop Proceedings, J. Stat. Phys. **54**, 1111-1540 (1989); J. García-Ojalvo, A. Hernández-Machado, and J. M. Sancho, Phys. Rev. Lett. **71**, 1542 (1993); A. Becker and L. Kramer, Phys. Rev. Lett. **73**, 955 (1994), and references therein.
- [13] I. Bialynicki-Birula, M. Cieplak, and J. Kaminski, *Theory of Quanta*, (Oxford University Press, New York, 1992); D. Bohm, *Quantum Theory*, (Dover Publications, New York, 1979).
- [14] P. Ramond, *Field Theory: A Modern Primer*, 2nd Ed. (Addison-Wesley, New York, 1990).
- [15] E. Brézin, in *Methods in Field Theory*, Les Houches 1975, Session XXVIII, ed. R. Balian and J. Zinn-Justin, (North-Holland, Amsterdam 1976).
- [16] E. Weinberg and A. Wu, Phys. Rev. D**36**, 2474, (1987).
- [17] M. Gleiser and R. Ramos, Phys. Rev. D**50**, 2441 (1994); B. L. Hu, J. P. Paz and Y. Zhang, in *The Origin of Structure in the Universe*, ed. E. Gunzig and P. Nardone (Kluwer Acad. Publ. 1993); D. Lee and D. Boyanovsky, Nucl. Phys. B**406**, 631 (1993); S. Habib, in *Stochastic Processes in Astrophysics*, Proc. Eighth Annual Workshop in Nonlinear Astronomy (1993).

ACKNOWLEDGMENTS

Julian Borrill was supported by a National Science Foundation grant no. PHY-9453431. Marcelo Gleiser was partially supported by the National Science Foundation through a Presidential Faculty Fellows Award no. PHY-9453431 and by a National Aeronautics and Space Administration grant no. NAGW-4270.

List of Figures

Figure 1. The time evolution of the mean field $\bar{\phi}(t)$ at five different lattice spacings $\delta x = 0.125, 0.25, 0.5, 1.0$ and 2.0 for the temperature independent potential — (a) without the renormalisation counterterms added (δx increasing downwards), and (b) with the renor-

malisation counterterms added.

Figure 2. The variation in the equilibrium mean field $\bar{\phi}_{\text{eq}}$ with the dimensionless temperature θ from the lattice (squares) and the continuum (lines) for the temperature independent potential — (a) for $M = 0.1$, (b) for $M = \sqrt{2}$, and (c) for $M = 10$.

Figure 3. The variation in the equilibrium mean field $\bar{\phi}_{\text{eq}}$ with the reduced dimensionless temperature θ_r from the lattice (squares) and the continuum (triangles) for the temperature independent potential. The dashed lines have slopes of $1/8$ and $1/2$.

Figure 4. The time evolution of the mean field $\bar{\phi}(t)$ at five different lattice spacings $\delta x = 0.125, 0.25, 0.5, 1.0$ and 2.0 for the temperature dependent potential — (a) without the renormalisation counterterms added (δx increasing downwards), and (b) with the renormalisation counterterms added.

Figure 5. The variation in the equilibrium mean field $\bar{\phi}_{\text{eq}}$ with the dimensionless temperature θ from the lattice (squares) and the continuum (lines) for the temperature dependent potential — (a) for $M = 0.1$, (b) for $M = \sqrt{2}$, and (c) for $M = 10$.

Figure 6. The variation in the equilibrium mean field $\bar{\phi}_{\text{eq}}$ with the reduced dimensionless temperature θ_r from the lattice (squares) and the continuum (triangles) for the temperature dependent potential. The dashed lines have slopes of $1/8$ and $1/2$.

Figure 1a

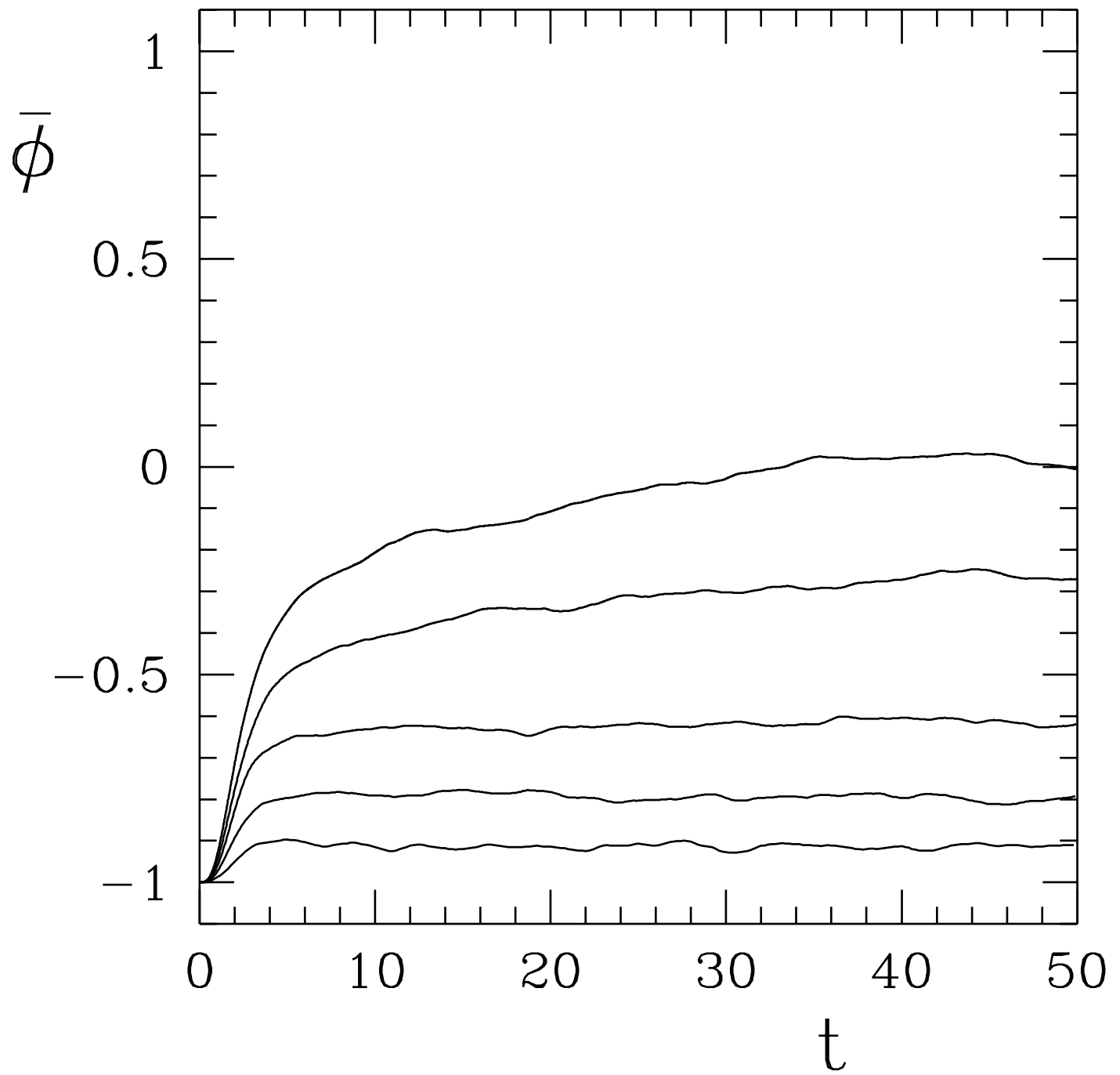


Figure 1b

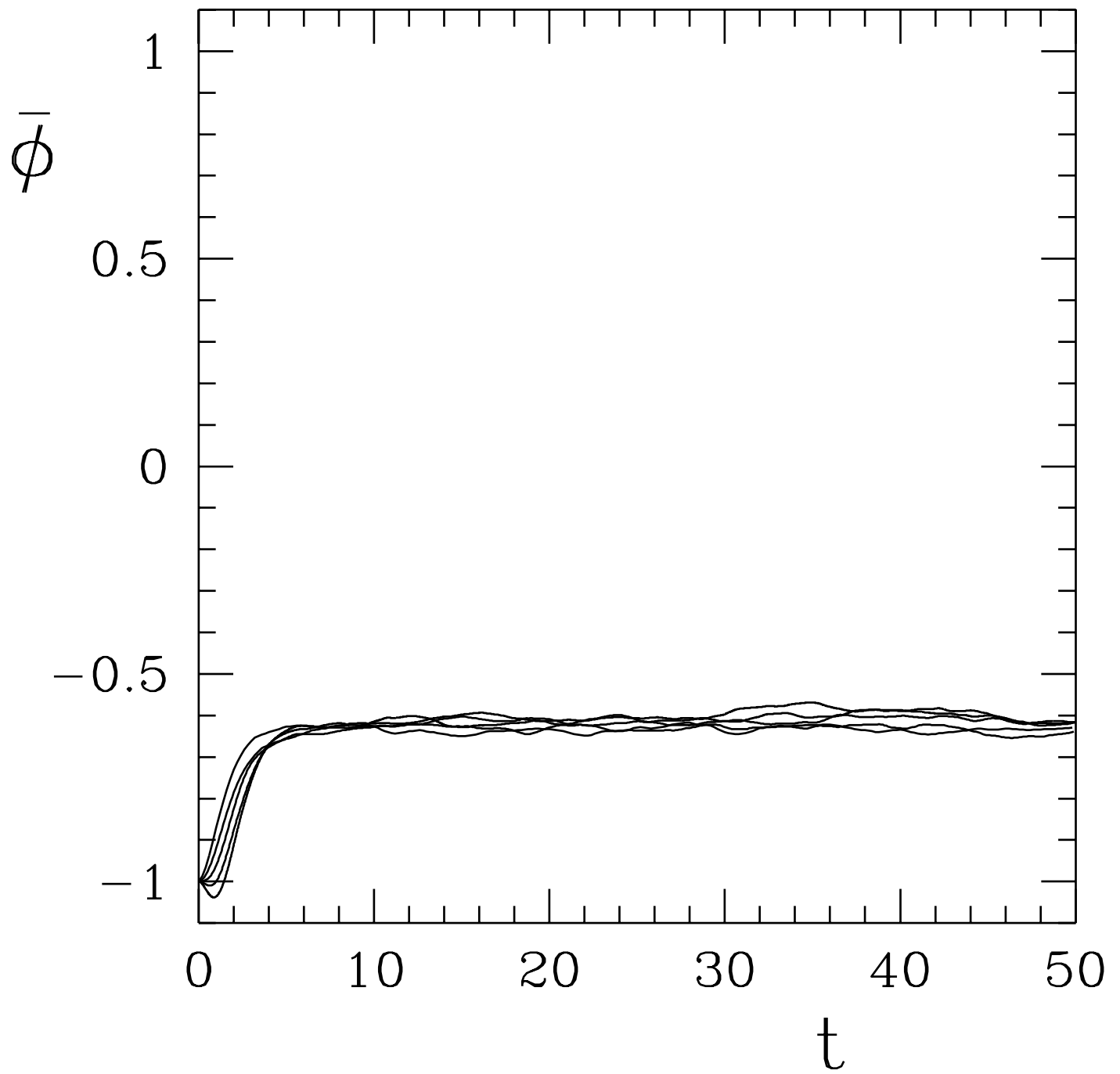


Figure 2a

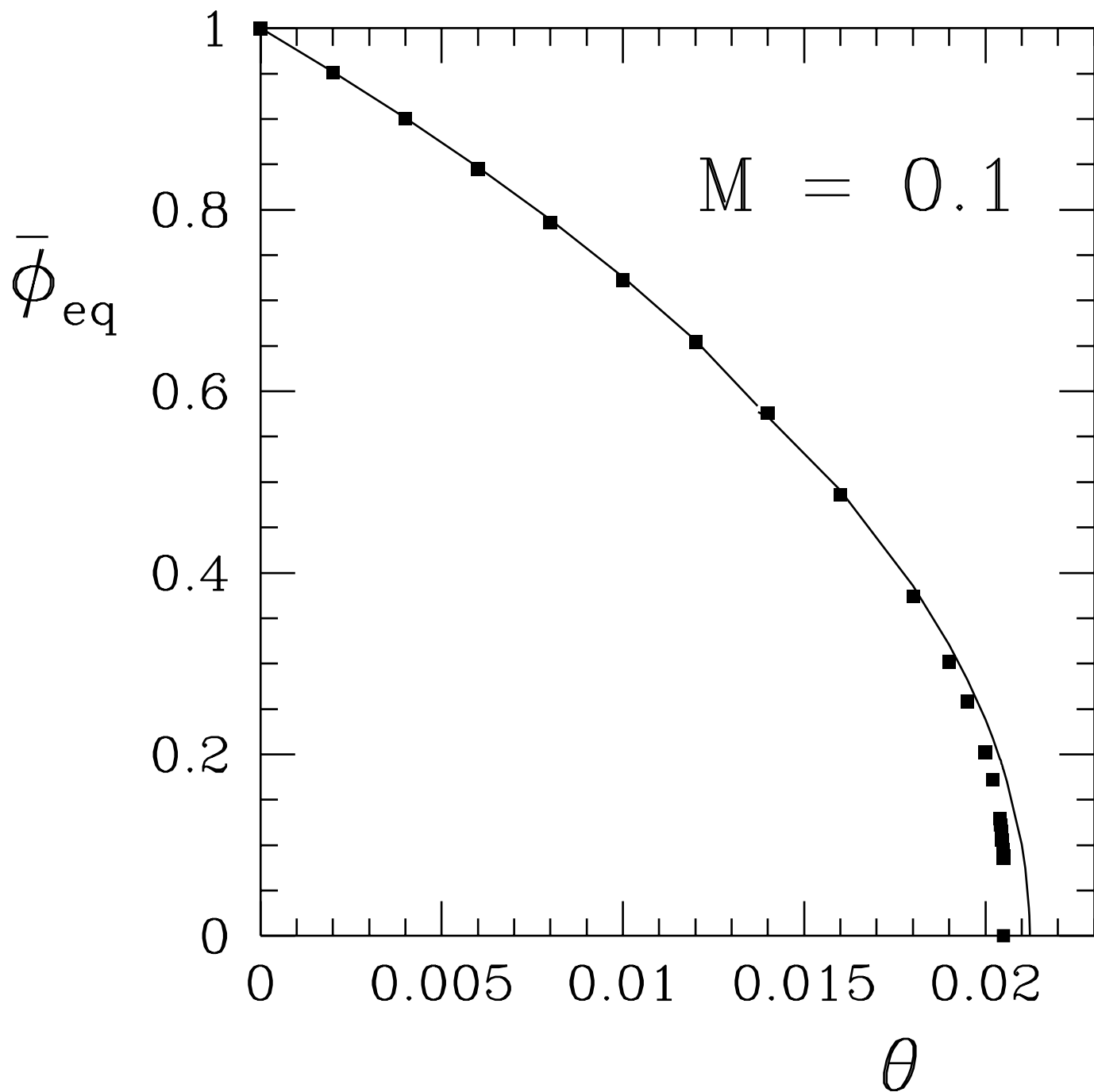


Figure 2b

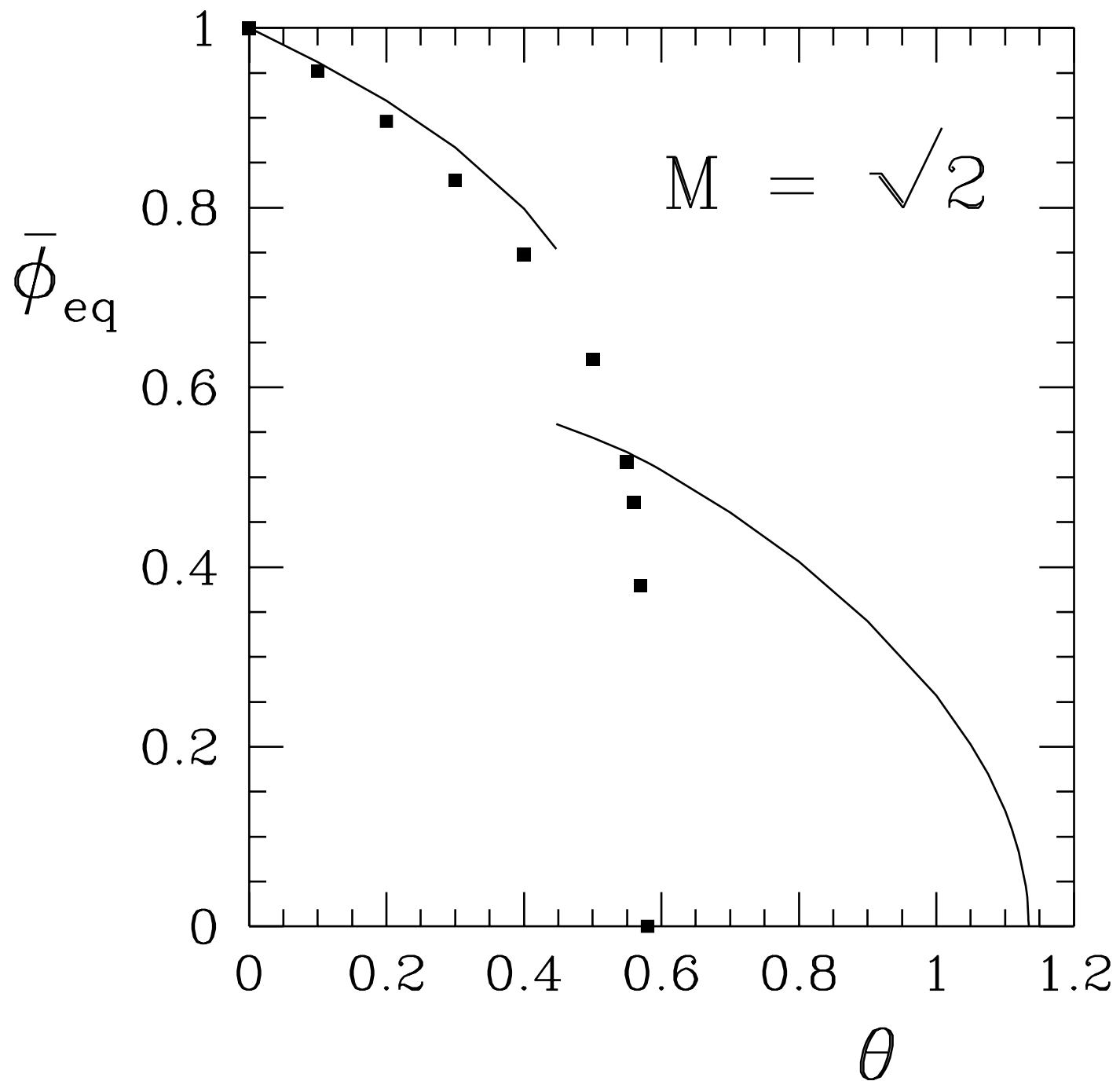


Figure 2c

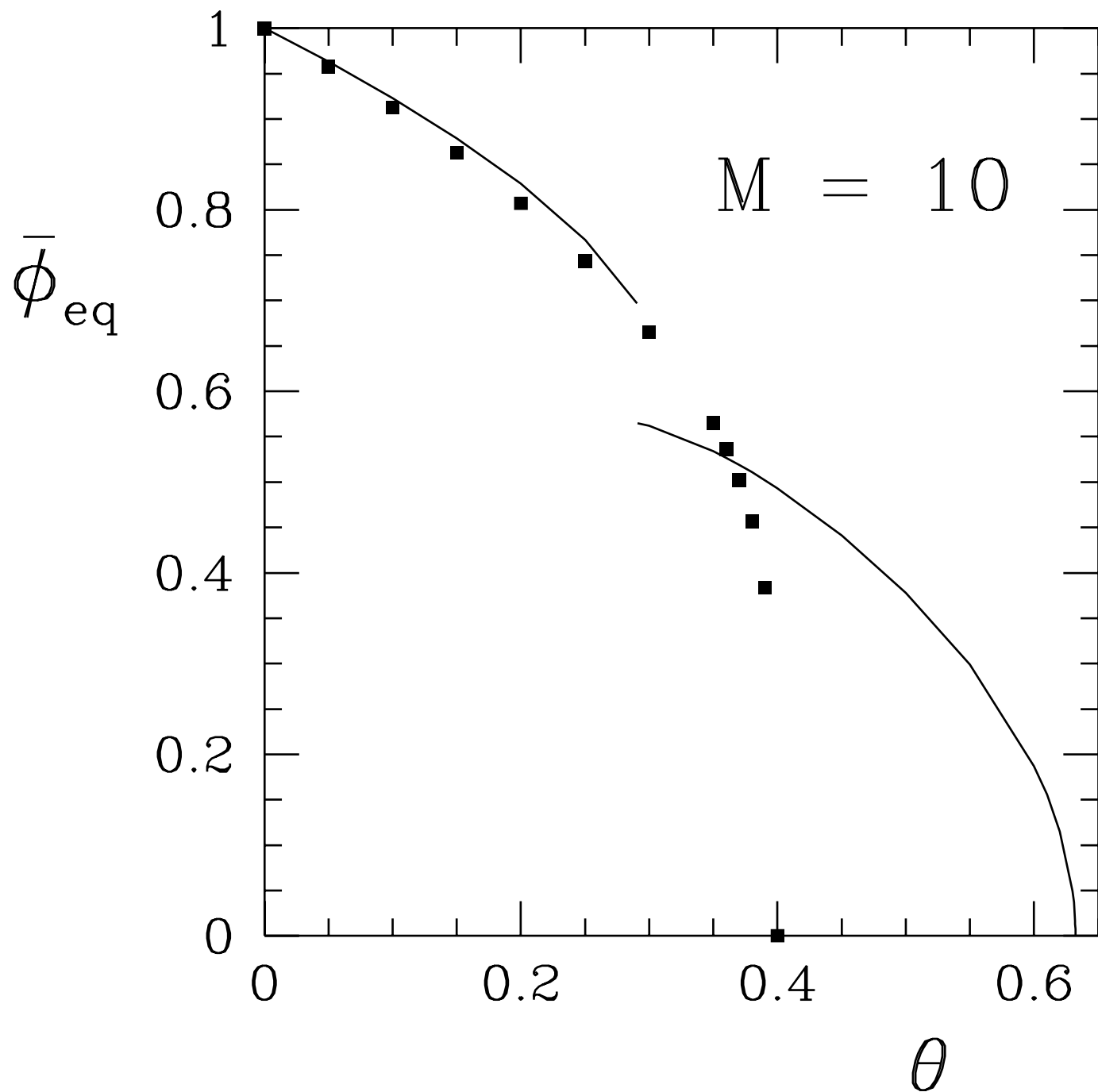


Figure 3

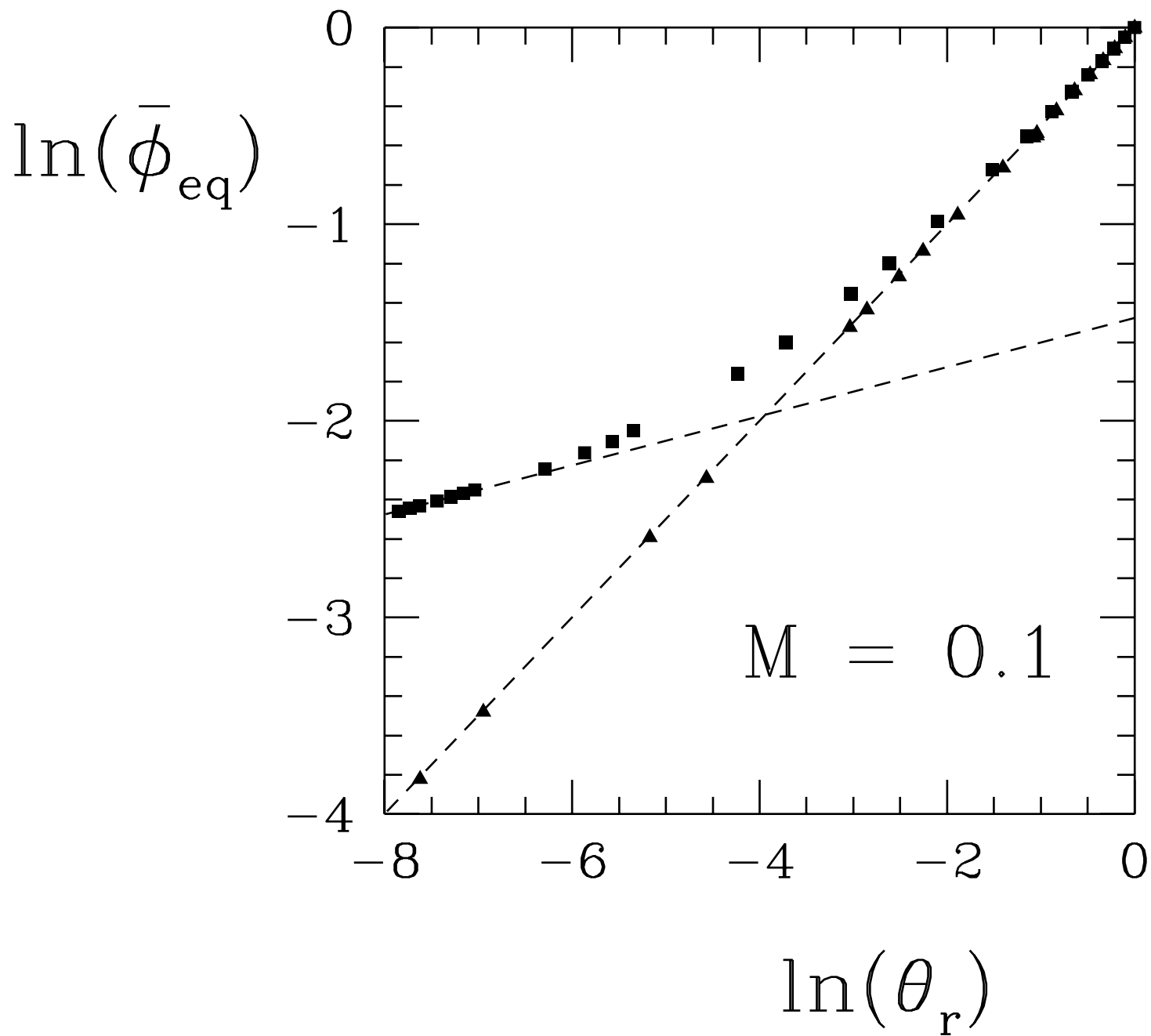


Figure 4a

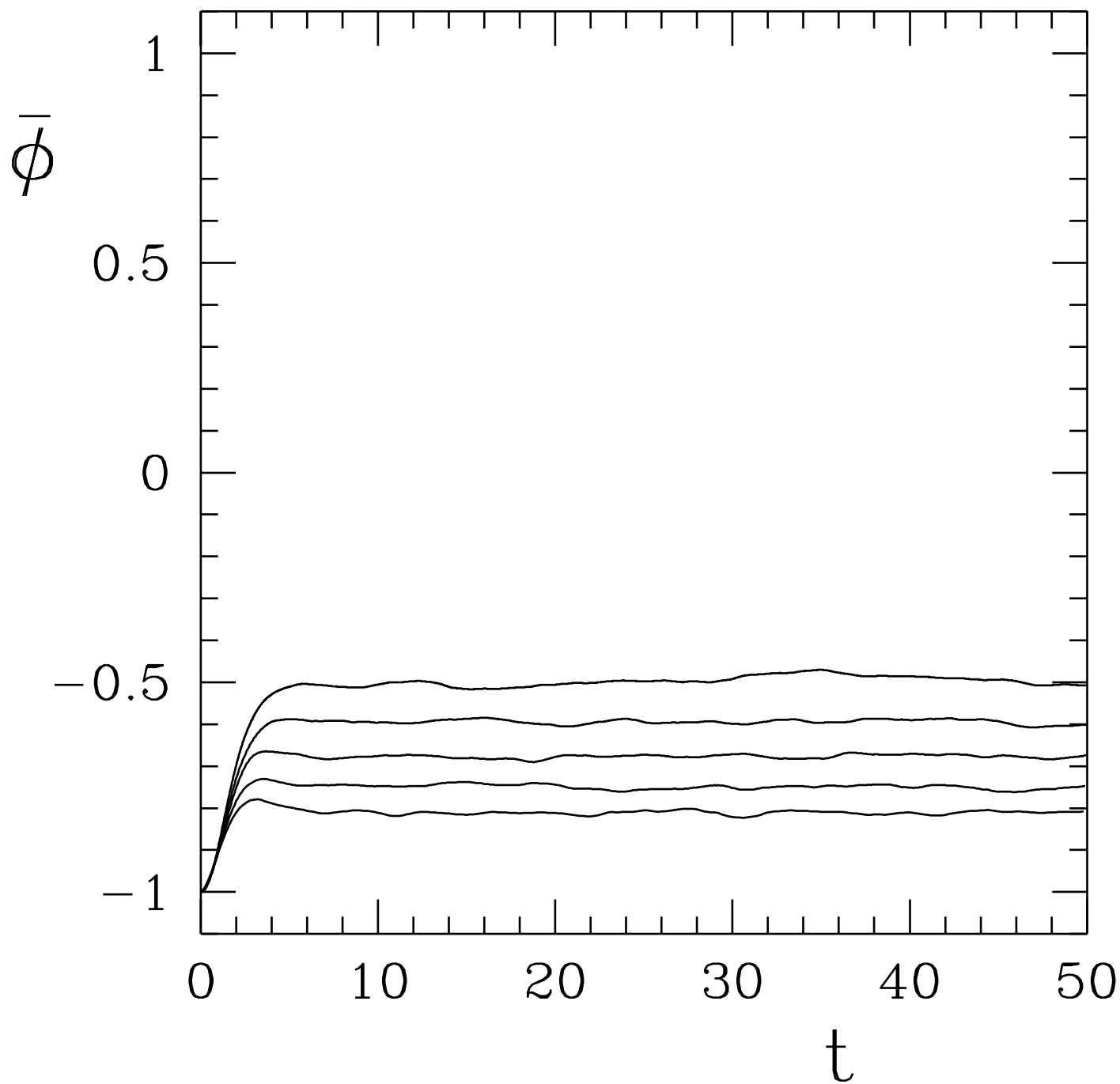


Figure 4b

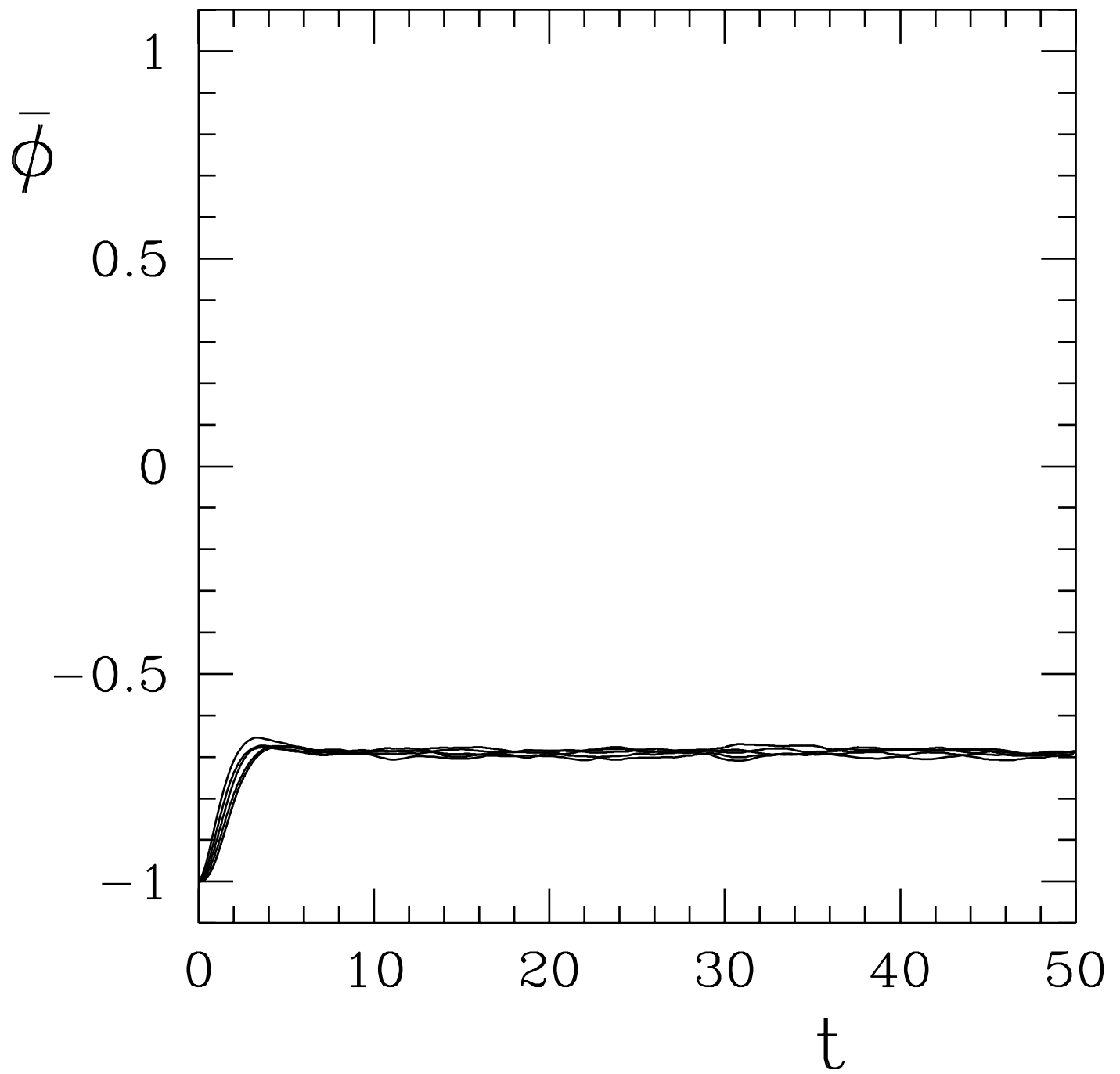


Figure 5a

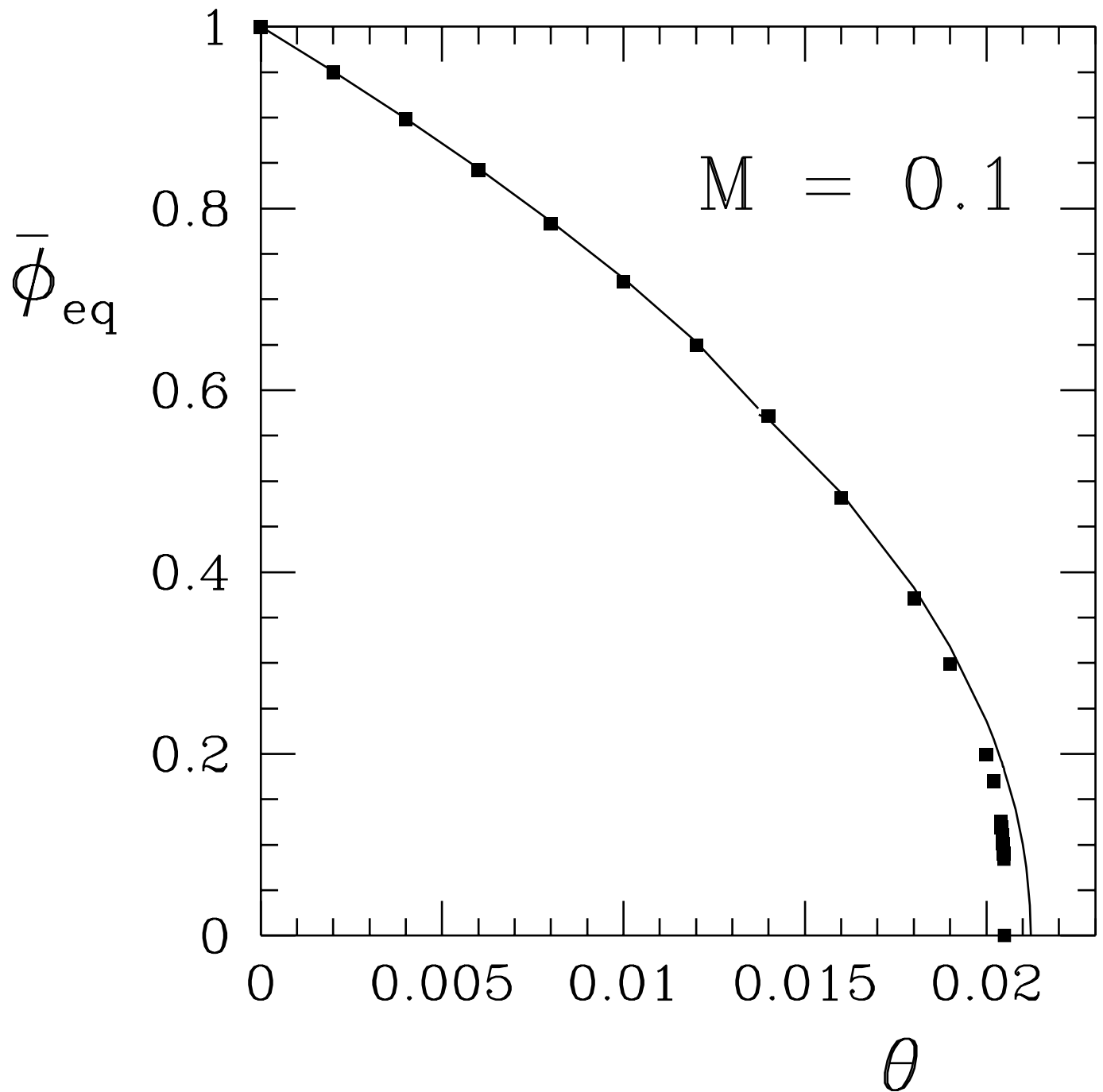


Figure 5b

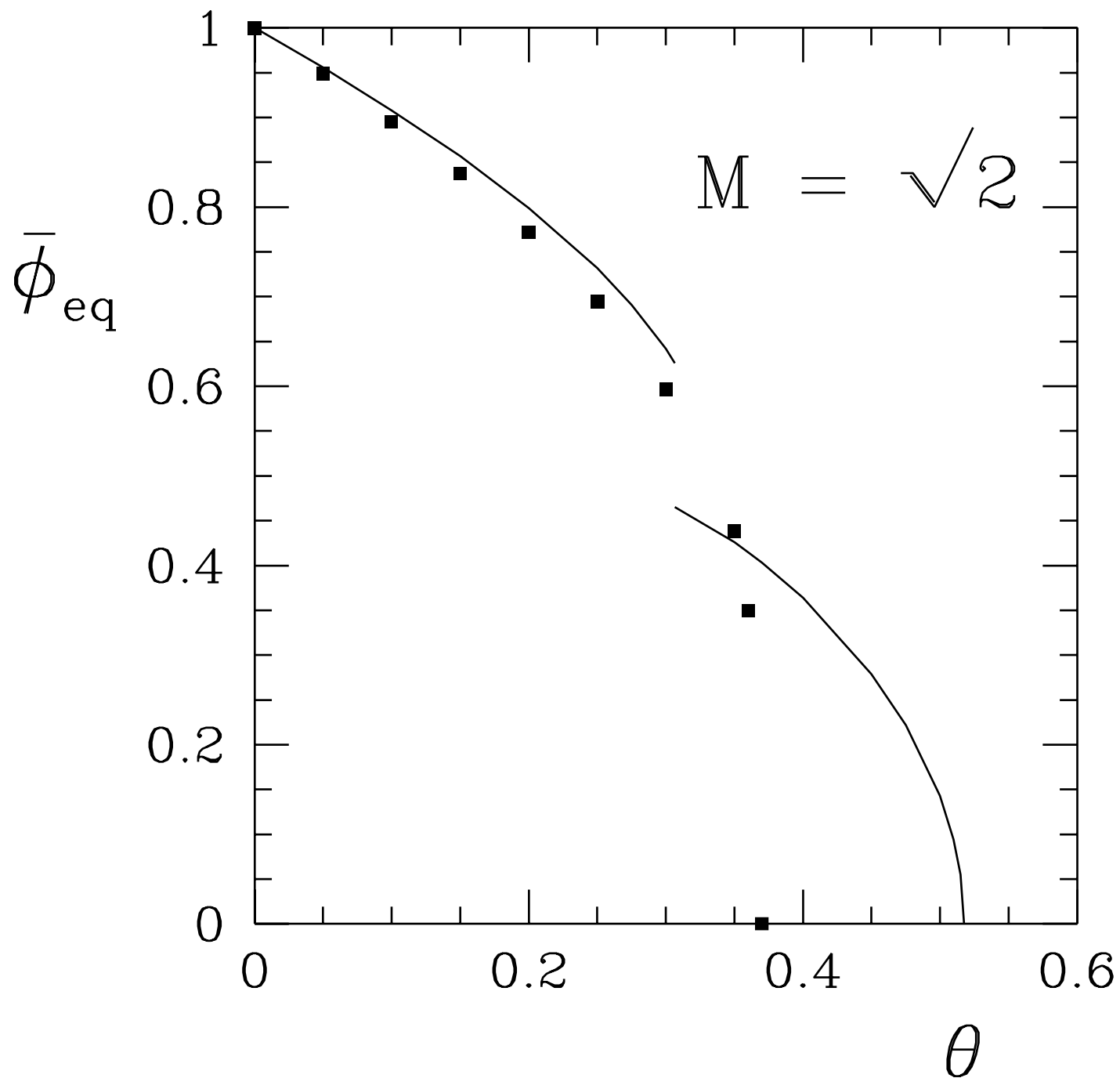


Figure 5c

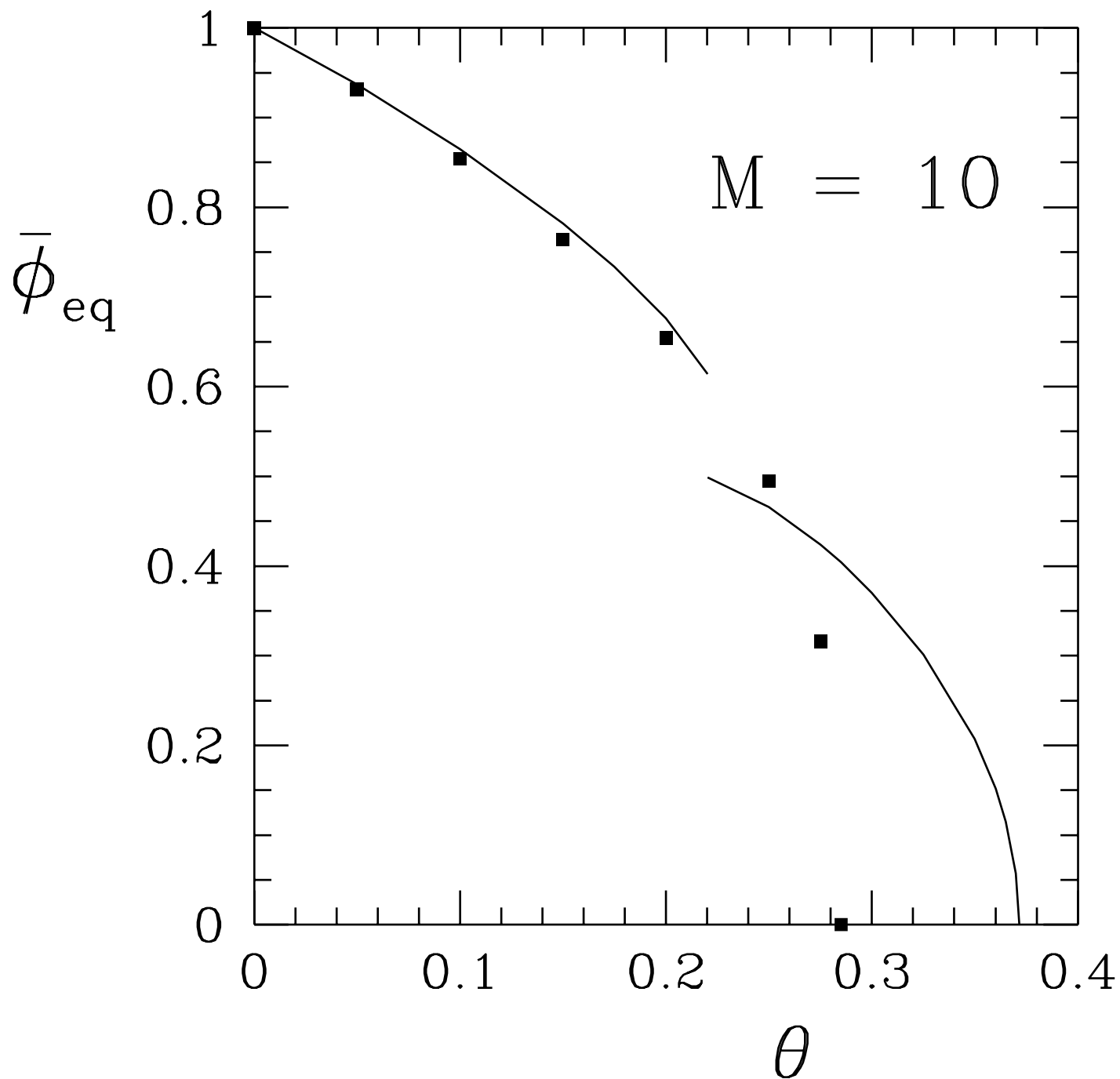


Figure 6

